

## RESEARCH ARTICLE

# MicroRNA858-mediated regulation of anthocyanin biosynthesis in kiwifruit (*Actinidia arguta*) based on small RNA sequencing

Yukuo Li<sup>☉</sup>, Wen Cui<sup>☉</sup>, Ran Wang, Miaomiao Lin, Yunpeng Zhong, Leiming Sun, Xiujuan Qi\*, Jinbao Fang\*

Zhengzhou Fruit Research Institute, Chinese Academy of Agricultural Sciences, Zhengzhou, P.R. China

☉ These authors contributed equally to this work.

\* [fangjinbao@caas.cn](mailto:fangjinbao@caas.cn) (JF); [qxixujuan@caas.cn](mailto:qxixujuan@caas.cn) (XQ)



## OPEN ACCESS

**Citation:** Li Y, Cui W, Wang R, Lin M, Zhong Y, Sun L, et al. (2019) MicroRNA858-mediated regulation of anthocyanin biosynthesis in kiwifruit (*Actinidia arguta*) based on small RNA sequencing. PLoS ONE 14(5): e0217480. <https://doi.org/10.1371/journal.pone.0217480>

**Editor:** Shin-Han Shiu, Michigan State University, UNITED STATES

**Received:** November 27, 2018

**Accepted:** May 13, 2019

**Published:** May 23, 2019

**Copyright:** © 2019 Li et al. This is an open access article distributed under the terms of the [Creative Commons Attribution License](https://creativecommons.org/licenses/by/4.0/), which permits unrestricted use, distribution, and reproduction in any medium, provided the original author and source are credited.

**Data Availability Statement:** All relevant data are within the manuscript and its Supporting Information files. All data were submitted to the database NCBI Sequence Read Archive (SRA accession: PRJNA515826).

**Funding:** This work was supported by the National Natural Science Foundation of China (Grant No. 31401825) to Xiujuan Qi and the Special Funds for Science and Technology Innovation Project of the Chinese Academy of Agricultural Sciences (CAAS-ASTIP-2017-ZFRI) to Jinbao Fang. The funders

## Abstract

As important regulators, miRNAs could play pivotal roles in regulation of fruit coloring. *Actinidia arguta* is a newly emerged fruit tree with extensively application prospects. However, miRNAs involved in *A. arguta* fruit coloring are unknown. In this study, *A. arguta* fruit were investigated at three developmental stages by small RNAs high-throughput sequencing. A total of 482 conserved miRNAs corresponding to 526 pre-miRNAs and 581 novel miRNAs corresponding to 619 pre-miRNAs were grouped into 46 miRNA families. Target gene prediction and analysis revealed that miR858, a strongly candidate miRNA, was involved in anthocyanin biosynthesis in which contributes to fruit coloring. The anthocyanin level was determined in three *A. arguta* cultivars by UPLC-MS/MS (ultra-performance liquid chromatography coupled with tandem mass spectrometry). In addition, qPCR (quantitative real-time PCR), cluster analysis were conducted as well as correlation analysis. All results were combined to propose a model in which describes an association of miRNA and anthocyanin biosynthesis in *A. arguta*. The data presented herein is the first report on miRNA profile analysis in *A. arguta*, which can provide valuable information for further research into the regulation of the miRNAs in anthocyanin biosynthesis and fruit coloring.

## Introduction

Domestication of kiwifruit (genus *Actinidia*, *Actinidiaceae*) began in the twentieth century [1]. It is known as the 'king of fruits' as it contains high contents of amino acids, mineral components, antioxidants, vitamin C and abundant dietary fiber [2]. Kiwifruit belongs to the genus of *Actinidia* and comprises approximately 54 species and 125 taxa [3]. Commercial cultivars are mainly selected from two species: *Actinidia chinensis* and *Actinidia deliciosa* due to their unique taste, large-fruit and long-storage [4]. Kiwifruit is traditionally known as a green-fleshed fruit for a long time until the release of yellow-fleshed kiwifruit. Recently, an all-red-fleshed kiwifruit (*A. arguta*) which appears in the red skin and the flesh is introduced to the

provided support in the form of salaries for all authors, but did not have any additional role in the study design, data collection and analysis, decision to publish, or preparation of the manuscript.

**Competing interests:** The authors have declared that no competing interests exist.

market. Consumers are attracted by its unique desirable agro characteristics such as appearance and high level of anthocyanin.

Anthocyanins, compose a group of flavonoids that are secondary metabolites and play important roles in the environmental adaptation [5], fruit development [6, 7], and even human health [8–11]. Anthocyanins are synthesized from a branch of flavonoids that also led to the synthesis of flavonols and proanthocyanidins [12]. The anthocyanin biosynthetic pathway has been extensively studied, and the majority of the structural and regulatory genes involved in anthocyanin accumulation have been isolated and identified in many model plants [13–23] and fruit species [24, 25]. The specific flow chart of anthocyanin biosynthetic pathway was also clearly drawn [26]. However, it is unclear what roles microRNAs (miRNAs) play in this process. Related studies were mainly focused on model plants, such as *Arabidopsis thaliana* [27] and *Solanum lycopersicum* [28], rarely in fruit trees, even less for kiwifruit.

As genome-encoded noncoding RNAs whose size ranges from approximately 18–24 nucleotides (nt), miRNAs play a crucial role in negatively regulating the expression of target genes via cleavage of complementary mRNAs or suppressing translation at the post-transcriptional level in eukaryotes [29, 30]. Plant miRNAs exert critical influence on the regulation of various biological processes, including development, primary and secondary metabolism and stress responses [30–33]. In recent years, several studies showed that miRNAs are involved in anthocyanin biosynthesis in *Arabidopsis*. The miR156 is a positive regulator which can repress the expression of *SPL9*, destabilizing the MBW transcriptional activation complex and thus preventing the expression of anthocyanin biosynthesis genes [32]. The miR408 is also a positive regulator, the over-expressed miR408 can increase anthocyanin accumulation in *Arabidopsis* seedlings [34, 35]. The miR858a positively regulates anthocyanin biosynthesis by repressing the *MYBL2* in *Arabidopsis* seedlings [27]. In contrast, miR828 or TAS4-siRNA81 (-) negatively regulate anthocyanin biosynthesis in *Arabidopsis* [36–38]. The miR858 negatively regulates anthocyanin biosynthesis in tomato (*Solanum lycopersicum*) [28]. However, the majority of studies investigating anthocyanin biosynthesis are concentrated in model plants, only a few studies investigated miRNAs in kiwifruit. The miR172 influences kiwifruit flowering by interacting with the floral gene *AP2* [39]. However, no study has investigated the involvement of miRNAs in anthocyanin biosynthesis of *A. arguta*.

To investigate the miRNAs regulated molecular mechanism controlling fruit coloring in *A. arguta*, the all-red-fleshed *A. arguta* cultivar ‘Hongbaoshixing’ (‘HB’, an all-red-fleshed tetraploid kiwifruit cultivar by wild selection.) was selected as an experimental material for small RNA high-throughput sequencing. In addition, three *A. arguta* cultivars ‘HB’, ‘Rubysihao’ (RB-4, an all-red-fleshed tetraploid kiwifruit) and ‘Huanyouyihao’ (‘HY-1’, an all-green-fleshed tetraploid kiwifruit) were used for anthocyanin measurement. Based on our data presented in this study, a regulatory model was established to show the association of miRNAs and anthocyanin biosynthesis in *A. arguta*. These findings provide evidence that the miRNAs play a regulatory role in the coloring process in *A. arguta* and also expand our knowledge in understanding the regulation mechanisms of anthocyanin biosynthesis.

## Materials and methods

### Fruit materials

All materials are maintained at the National Kiwifruit Germplasm Garden of the Zhengzhou Fruit Research Institute, Chinese Academy of Agricultural Sciences, Henan Province, China. For small RNA sequencing, the fruits of the all-red-fleshed *A. arguta* cultivar ‘HB’ was harvested at three developmental stages, the dates of harvesting were recorded as days after full bloom (DAFB), including the S1 stage, at 70 DAFB (green fruit); the S2 stage, at 100 DAFB

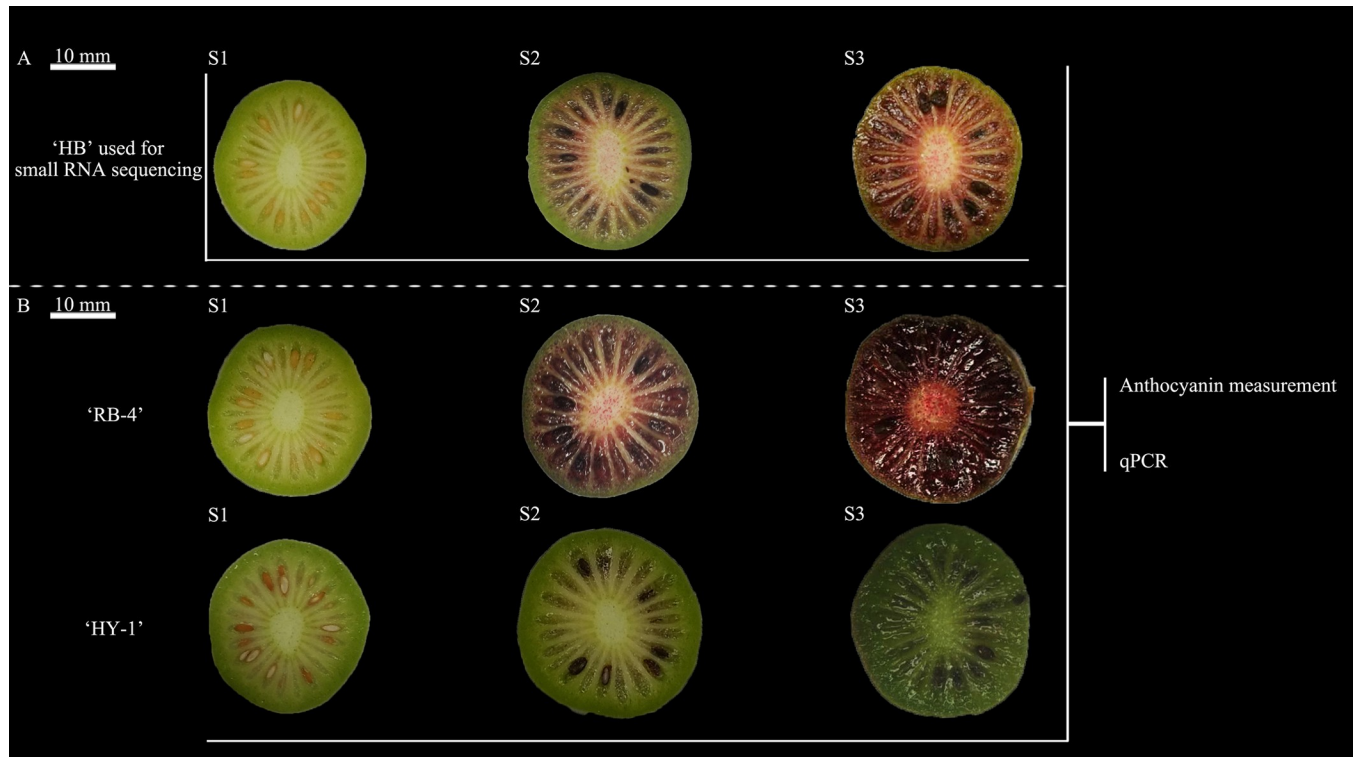


**Fig 1. Change in fruit color at three stages: S1, S2 and S3.** (A) Color change in all-red-fleshed kiwifruit 'HB'. (B) Color change in all-red-fleshed kiwifruit 'RB-4' and all-green-fleshed kiwifruit 'HY-1'. 'HB' was used for small RNA sequencing. 'HB', 'RB-4' and 'HY-1' were used for anthocyanin measurement and qPCR.

<https://doi.org/10.1371/journal.pone.0217480.g001>

(the color-break stage, beginning to turn red); and the S3 stage, at 125 DAFB (ripe red fruit and also the stage of harvest maturity) (Fig 1A). In each stage, fruit samples used for small RNA sequencing were randomly collected from six different trees, every two of which served as a biological replication; thus, three independent biological replicates were included throughout the sequencing process. For anthocyanin content analysis and gene expression profiling, the fruits of 'HB' were harvested at different stages. 'RB-4' (an all-red-fleshed *A. arguta* kiwifruit cultivar) and 'HY-1' (an all-green-fleshed kiwifruit cultivar) were also included for this analysis (Fig 1B). The fruit was dissected using a blade, frozen immediately in liquid nitrogen, and then stored at  $-80^{\circ}\text{C}$  until further use.

### Total RNA isolation, small RNA library construction, and sequencing

The total RNA was extracted using Trizol reagent (Invitrogen, CA, USA) in accordance with the manufacturer's procedure. The total RNA quantity and purity were analyzed using a 2100 Bioanalyzer and an RNA 6000 Nano LabChip Kit (Agilent, CA, USA) with an RNA integrity number (RIN)  $>7.0$ . Approximately  $1\ \mu\text{g}$  of the total RNA was used to prepare small RNA libraries in accordance with the protocol of a TruSeq Small RNA Sample Prep Kit (Illumina, San Diego, USA). In addition, single-end sequencing (36 bp) was performed on an Illumina HiSeq 2500 at LC-BIO Company, Hangzhou, China. All sequencing was performed in triplicate.

### Data processing

The raw data reads were subjected to an Illumina pipeline filter (Solexa 0.3), and after which the dataset was further processed with an in-house program, ACGT101-miR (LC Sciences,

Houston, Texas, USA) to remove adapter dimers, junk, low complexity, common RNA families (rRNA, tRNA, snRNA, and snoRNA) and repeats. Those unique sequences with a length in 18–25 nt were subsequently mapped to specific species precursors using miRBase 20.0 (<http://www.mirbase.org/>) by BLAST queries to identify both known miRNAs and novel 3p- and 5p-derived miRNAs. Variation in length at both 3' and 5' ends and one mismatch within the sequence were allowed in the alignment. Those unique sequences that mapped to the hairpin arms of the mature miRNAs of specific species were identified as known miRNAs; those unique sequences that mapped to the other hairpin arms of the precursors of known specific species (opposite that of the annotated mature miRNA-containing arm) were considered novel 5p- or 3p-derived miRNA candidates. The remaining sequences were mapped to other selected species precursors (excluding specific species) in miRBase 20.0 by BLAST queries, and to determine their genomic locations, the mapped pre-miRNAs were further BLASTed against the genomes of specific species. We defined the above two miRNA sequences as known miRNAs. The unmapped sequences were BLASTed against the specific genomes, and the RNA hairpin structures containing sequences were predicted from the 120 nt flanking sequences using RNAfold software (<http://rna.tbi.univie.ac.at/cgi-bin/RNAfold.cgi>).

### Quality control of biologically repeated samples and sequencing data

For biologically repeated samples, correlations of gene expression levels between different samples constitute an important indicator for testing both the reliability of experiments and the reasonability of sample selection; hence, correlation analyses between every two samples were conducted using Person correlation coefficients that were calculated using R Language [40]. In addition, principal component analysis (PCA) was used to examine the distribution of data and verify the reasonability of the experimental design. Finally, all data were submitted to the database NCBI Sequence Read Archive (SRA accession: PRJNA515826).

### Analysis of differentially expressed miRNAs

To determine the expression levels of miRNAs, the differential expression of miRNAs was analyzed by Chi square (N×N) tests; this analysis was performed on the basis of normalized deep-sequencing counts that were normalized as transcripts per million (TPM) using the formula  $\text{normalized expression} = \text{mapped read count} / \text{total reads} * 10^6$  [41]. All differential expression between two samples was analyzed using the DEGseq R package [42]; the significance threshold for each test was set to be 0.01.

### Target gene prediction and enrichment analysis

Based on target penalty strategy, TargetFinder software was used to predict the putative target genes of miRNAs identified in this study [43]. In conjunction with the Gene Ontology (GO) and Kyoto Encyclopedia of Genes and Genomes (KEGG) information on kiwifruit (*A. chinensis*), GO functional annotation and KEGG signal pathway annotation for the differentially expressed miRNAs were carried out. All GO and KEGG pathway annotation for the predicted target genes of the differentially expressed miRNAs were subjected to Fisher's accurate hypothesis tests, and, every GO and KEGG annotation was subjected to an enrichment analysis [44, 45].

### Measurements of anthocyanin contents

For 'HB', 'RB-4' and 'HY-1', 10 g of flesh tissue per sample was ground and then extracted in a solution consisting of anhydrous ethanol, hydrochloric acid and water (volume ratio-2:1:1)

twice by ultrasonic techniques. The anthocyanin components were qualitatively and quantitatively analyzed using UPLC-MS/MS (ultra-performance liquid chromatography coupled with tandem mass spectrometry) (Agilent, Palo Alto, CA, USA). Cyanidin (CAS: 528-58-5; chromatographic purity >98%; Chromadex), delphinidin (CAS: 528-53-0; chromatographic purity >96%), cyanidin-3-O-galactoside (CAS: 27661-36-5; chromatographic purity >98%; Chromadex) and delphinidin-3-O-galactoside (CAS: 28500-00-7; chromatographic purity >95%; Chromadex) were used as authentic standard samples for constructing a standard curve and for single point quantitation. Total anthocyanin content was measured using Plant Anthocyanin Content Detection Kit (Solarbio, Beijing, China) following manufacture's recommendations. Each sample was analyzed in triplicate.

### Expression analysis by qPCR (quantitative real-time PCR)

The total RNA was isolated from the flesh samples of the three different cultivars at three different stages using the modified cetyltrimethyl ammonium bromide (CTAB) method [46]. One microgram of total RNA was used for cDNA synthesis with a RevertAid First Strand cDNA Synthesis Kit (Thermo Fisher Scientific, MA, USA). The reaction mixture and qPCR program used were in accordance with those described previously [47]. All analyses were repeated three times using biological replicates. In addition, the relative expression levels were calculated using the  $2^{-\Delta\Delta C_t}$  method [48].

### Expression profiling of miR858 in red-fleshed and green-fleshed kiwifruit

The total RNA extraction of red-fleshed 'HB' and green-fleshed 'HY-1' at three developmental stages was carried out according to the Quick RNA Isolation Kit (Huayueyang Biotech, Beijing, China). Two hundred nanogram of total RNA was used for cDNA synthesis with TransScript miRNA First-Strand cDNA Synthesis SuperMix Kit (TransGen Biotech, Beijing, China). Quantitative real-time PCR was carried out using LightCycler 480 System (Roche Diagnostics). Thermal cycling conditions were 94°C for 30 sec, then 45 cycles of 94°C for 5 sec, 60°C for 15 sec and 72°C for 10 sec, which was described as 3 step protocol in TransStrat Tip Green qPCR SuperMix Kit (TransGen Biotech, Beijing, China). The 5S rRNA [27] was considered as the control gene for normalization. Three replicates were carried out for each analysis.  $2^{-\Delta\Delta C_t}$  method was used to calculate relative expression level [48].

### Statistical analysis

Statistical analyses were performed using GraphPad Prism 5 (GraphPad Software Inc., San Diego, CA, USA), and cluster analyses were performed using both R-3.4.2 and TMEV software [49]. IBM SPSS Statistics 20 was used to test significant differences. Each value represents mean  $\pm$  SD of three independent biological replicates.

## Results

### Quality control and overview of deep sequencing of small RNA

The 'HB' kiwifruit at three developmental stages was used for small RNA high-throughput sequencing. To ensure the reliability of the sequencing results, strict quality control was applied in this study. Person correlations and PCA between different samples verified the reliability of the data and the reasonability of the experimental design (S1 and S2 Figs). To identify possible miRNAs involved in the fruit development of 'HB', three independent small RNA libraries from 'HB' kiwifruit at three developmental stages were constructed and sequenced by high-throughput Illumina Solexa system. A total of 15,373,860 raw reads were obtained by

sequencing. After removing the 3' adapter sequences, reads whose length was < 18 nt and consecutive nucleotide dimers and trimer, 11,193,696 clean reads represented by 7,364,610 unique tags were selected (Table 1). The length distribution of clean reads and unique tags showed that the majority (96.0% for clean reads, 97.6% for unique tags) were 21–25 nt and the predominant sequences were 24 (60.5% for clean reads, 69.8% for unique tags) nt in length, followed by 23 nt and 22 nt (Fig 2A). This is consistent with the typical characteristics of Dicer enzyme cleavage.

## MiRNAs identification

To identify the conservative and novel miRNAs in the 'HB' flesh, the small RNA sequences were mapped to other plant miRNAs in the miRBase database. A total of 482 conservative miRNAs corresponding to 526 pre-miRNAs and a total of 581 novel miRNAs corresponding to 619 pre-miRNAs were identified (Table 2). The majority of these miRNAs were highly homologous to those in other plants, including *Glycine max*, *Populus trichocarpa*, *Malus domestica*, *Manihot esculenta* and *Vitis vinifera*. One hundred seventy-five miRNAs were identified in the 'HB' that homologous to those in *Glycine max* (Fig 2B). The sequences similarity revealed that these miRNAs were grouped into 46 miRNA families (S1 Table). Of these 46 miRNA families, six miRNA families including miR156, miR166, miR167, miR172, miR396 and miR398, were conserved in 32, 30, 27, 29, 32 and 25 plant species, respectively. The majority of the miRNAs were not conserved and has been only identified in one species. With the exceptions of miR862, miR2592, miR5645, miR6476 and miR7122, only one member was found in the remaining miRNA families (S2 Table).

## Prediction and analysis of miRNA targets

To better understand the biological function of the miRNAs obtained above, target genes for 321 identified miRNAs whose expression significantly differed (S3 Table) were predicted by TargetFinder software. The information of the predicted target genes included the miRNA ID, transcript ID, gene ID, score, range, strand, GO annotation and KEGG annotation (S4 Table). To obtain more detailed information about the function of the identified miRNAs, the predicted target genes were subjected to GO analysis (S5 Table). A total of 814 target genes were

**Table 1. Overview of reads from raw data to cleaned sequences.**

Type	Count	Percentage/%
Raw reads	15,373,860	100.000
3ADT&length filter	3,113,309	20.332
Junk reads	125,613	0.806
Rfam	528,255	3.484
mRNA	617,070	4.081
Repeats	7,735	0.052
Clean reads	11,193,696	72.654

Note: 3ADT&length filter: reads removed due to 3ADT not found and length with <18 nt and >25 nt were removed. Junk reads: Junk: > = 2N, > = 7A, > = 8C, > = 6G, > = 7T, > = 10Dimer, > = 6Trimer, or > = 5Tetramer. Rfam: Collection of many common non-coding RNA families except microRNA; <http://rfam.janelia.org>. Repeats: Prototypic sequences representing repetitive DNA from different eukaryotic species; <http://www.girinst.org/repbase>. Notes: valid reads may not be equal to raw reads - 3ADT&length, filter, Junk reads, mRNA, Rfam, Repeats, because there are overlapped sequences between mRNA, Rfam and Repeats. mRNA\_Database: <http://bioinfo.bti.cornell.edu/cgi-bin/kiwi/blast.cgi>

<https://doi.org/10.1371/journal.pone.0217480.t001>

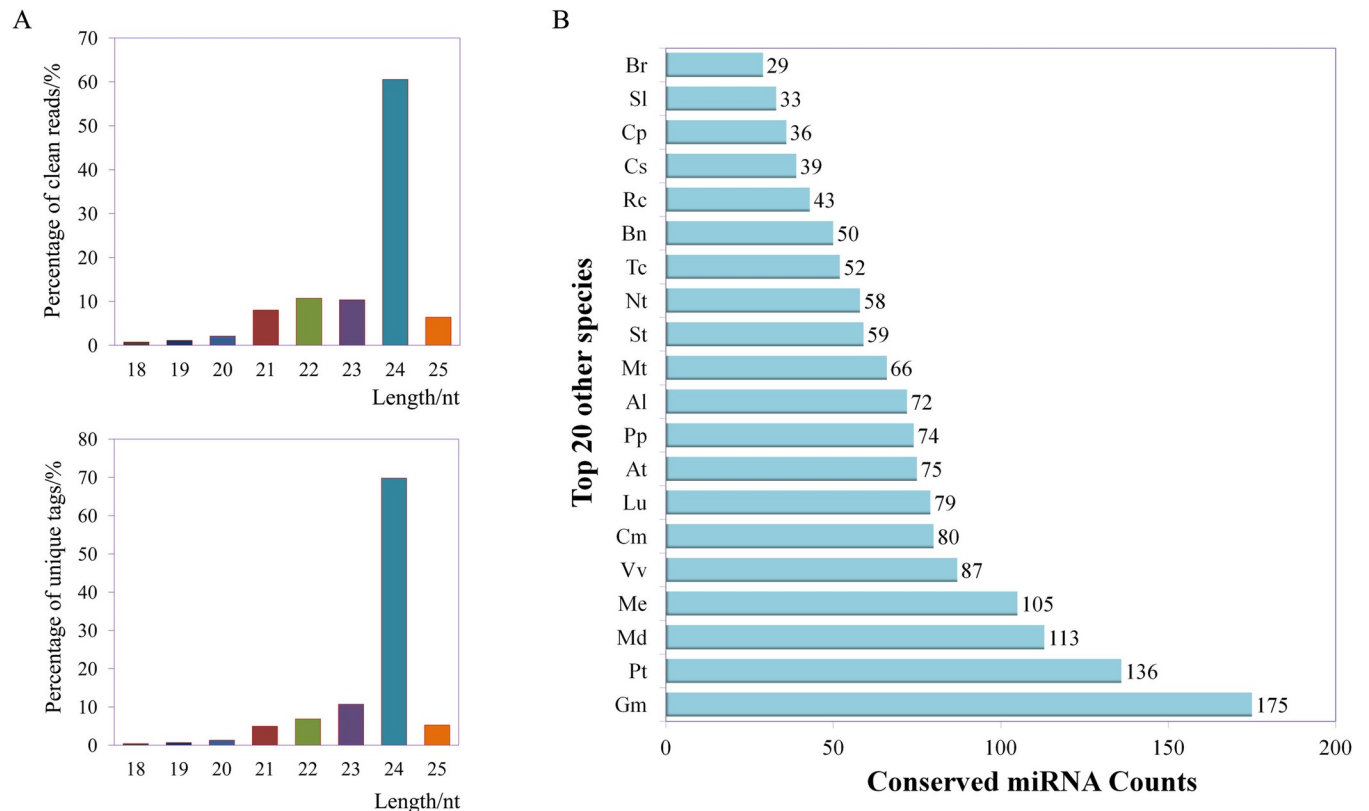


**Fig 2. Analysis of sequence length and conservation of miRNAs.** (A) Distribution of small RNAs with different sequence length according to clean reads and unique tags. (B) Conservation of the identified miRNAs with those in other species. The x-axis represents the number of conserved miRNAs and the y-axis indicates the top 20 number in other species. Different prefixes indicating different species are as follows: Br-*Brassica rapa*; Sl-*Solanum lycopersicum*; Cp-*Carica papaya*; Cs-*Citrus sinensis*; Rc-*Ricinus communis*; Bn-*Brassica napus*; Tc-*Theobroma cacao*; Nt-*Nicotiana tabacum*; St-*Solanum tuberosum*; Mt-*Medicago truncatula*; Al-*Arabidopsis lyrata*; Pp-*Prunus persica*; At-*Arabidopsis thaliana*; Lu-*Linum usitatissimum*; Cm-*Cucumis melo*; Vv-*Vitis vinifera*; Me-*Mamihot esculenta*; Md-*Malus domestica*; Pt-*Populus trichocarpa*; Gm-*Glycine max*.

<https://doi.org/10.1371/journal.pone.0217480.g002>

classified into three functional categories: biological processes, cellular components and molecular function, each of which contained 25, 15 and 10 GO terms, respectively (Fig 3A). Among those target genes, 129, 69 and 26 were assigned to 'protein binding' (GO: 0005515), 'regulation of transcription' (GO: 0006355) and 'metabolic process' (GO: 0008152), respectively. In addition, KEGG Pathway analysis was performed (S6 Table) and showed that 207 target genes were assigned into 18 pathway terms (Fig 3B), which were significantly related to response to 'calcium-binding protein CML' (ko04626) and 'acetyl-CoA C-acetyltransferase' (ko01200).

### Candidate miR858 involved in anthocyanin biosynthesis

Our study focuses on anthocyanins which can lead to fruit coloring. We are interested in identifying candidate miRNAs that contributes to the anthocyanin synthesis. Because of the phenotypic difference of 'HB' fruit color between S1 (fruit is green) and S3 (fruit is completely red) was the most obvious, so the comparison of S3 vs S1 was served as the cut-in spot for analysis. The results for conserved miRNAs with significantly expressed difference in comparison of S3 vs S1 showed that 17 conserved miRNAs were up-regulated and 10 conserved miRNAs were down-regulated, respectively (Fig 4A). Furthermore, the target genes of these miRNAs were

**Table 2. Summary of conservative and novel miRNAs.**

Groups	Type	Pre-miRNA	Unique miRNA
Gp1	Conservative	33	49
Gp2a		164	175
Gp2b		295	223
Gp3		34	35
	Total conservative	526	482
Gp4	Novel	619	581
	Total	1,145	1,063

Note: Gp1 indicates reads map to specific miRNAs/pre-miRNAs in miRbase and the pre-miRNAs further map to the genome & EST; Gp2a indicates reads map to selected miRNAs/pre-miRNAs in miRbase. The mapped pre-miRNAs do not map to the genome, but the reads (and of course the miRNAs of the pre-miRNAs) map to genome. The extended genome sequences from the genome loci may form hairpins; Gp2b indicates reads were mapped to miRNAs/pre-miRNAs of selected species in miRbase and the mapped pre-miRNAs were not further mapped to genome, but the reads (and of course the miRNAs of the pre-miRNAs) were mapped to genome. The extended genome sequences from the genome loci may not form hairpins. Gp3 indicates reads map to selected miRNAs/pre-miRNAs in miRbase. The mapped pre-miRNAs do not map to the genome, and the reads do not map to the genome. Gp4 indicates reads do not map to selected pre-miRNAs in miRbase. But the reads map to genome & the extended genome sequences from genome may form hairpins.

<https://doi.org/10.1371/journal.pone.0217480.t002>

also predicted and identified. The number of target genes for individual miRNAs varies from 1 to 62. For instance, miR858 tops the list with 62 target, followed by miR166i and miR2586a, which have 23 and 20 targets, respectively (Fig 4B). Among these targets, only c105731\_g1 (named *AaMYBC1*) which is the target of miR858 was related with anthocyanin biosynthesis (S7 Table), which guided us to take miR858 as the object for next study.

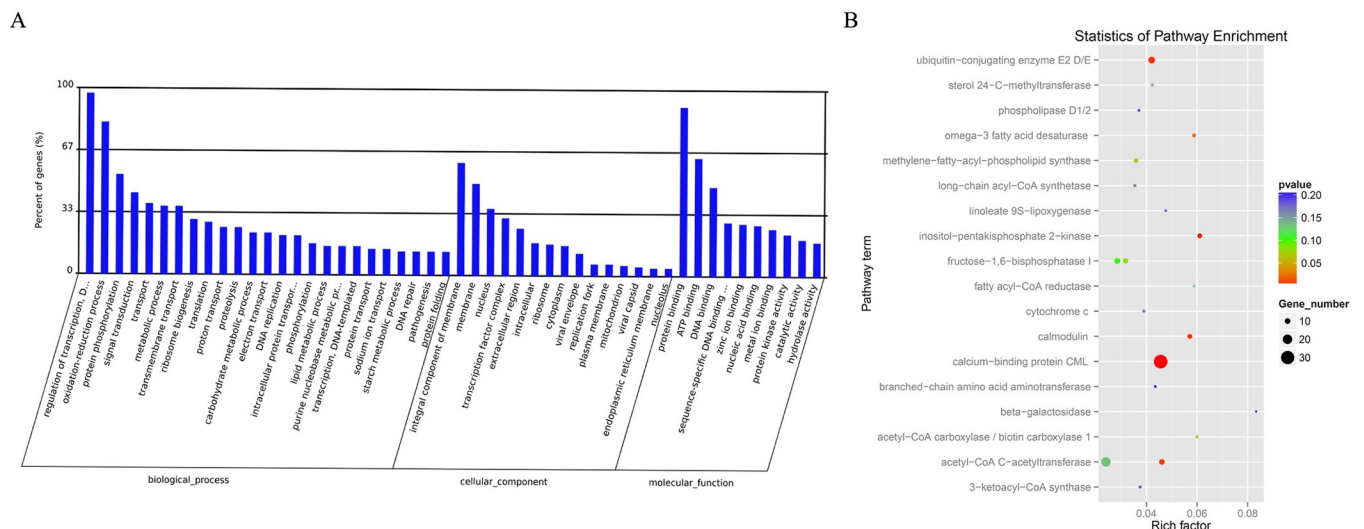


**Fig 3. GO and KEGG analysis for miRNAs.** (A) GO classification of target genes. Eight hundred fourteen target genes were assigned to three GO categories: 25, 15, and 10 GO terms were categorized as biological process, cellular components, and molecular functions, respectively. The x-axis represents the GO terms belonging to three GO categories, and the y-axis indicates the percent of genes. (B) KEGG pathway enrichment scatter plot. The horizontal axis represents the rich factor corresponding to the pathway, and the vertical axis represents the pathway name. P-values are represented by the color of the points. The number of genes with in each pathway is indicated by the size of point.

<https://doi.org/10.1371/journal.pone.0217480.g003>

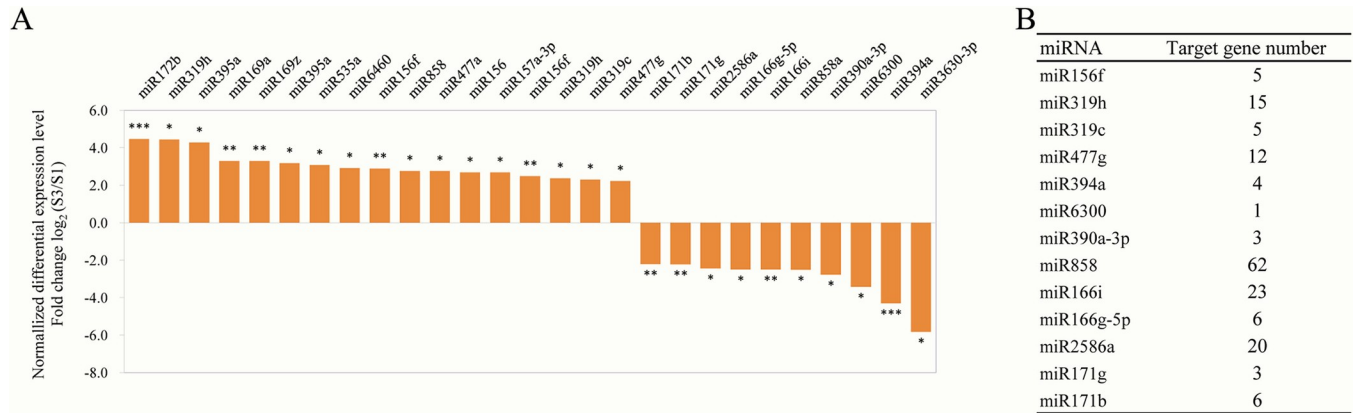


**Fig 4. The miRNAs with significantly expressed difference and their target genes in comparison S3 vs S1.** (A) Up-regulated and down-regulated miRNAs, (B) Target gene number of 13 miRNAs. Statistical significance: \* $P < 0.05$ , \*\*  $P < 0.01$ , \*\*\*  $P < 0.001$ .

<https://doi.org/10.1371/journal.pone.0217480.g004>

### Analysis of anthocyanin components and content

To investigate the relationship between fruit color and anthocyanin components and content, three different *A. arguta* cultivars ('HB', 'RB-4' and 'HY-1') were served as materials and four different anthocyanin types were served as standard for measuring anthocyanin components and content (S3 Fig). In the flesh tissues of the three *A. arguta* cultivars, these four anthocyanin components were detected in 'HB' and 'RB-4'. Except for cyanidin-3-O-galactoside, the remaining three components were detected in 'HY-1', but the content was extremely low. Cyanidin and delphinidin content at S1 were higher than that at S3 in 'HB' and 'RB-4', whereas cyanidin-3-O-galactoside content was just the opposite (Fig 5), which indicate the cyanidin-3-O-galactoside was the main chromogenic pigment in *A. arguta* and also suggest that it is just because of the existence of cyanidin-3-O-galactoside leading to color differences between red and green-fleshed *A. arguta* cultivars. The changing trend of total anthocyanin content at three stages was similar with that of cyanidin-3-O-galactoside.

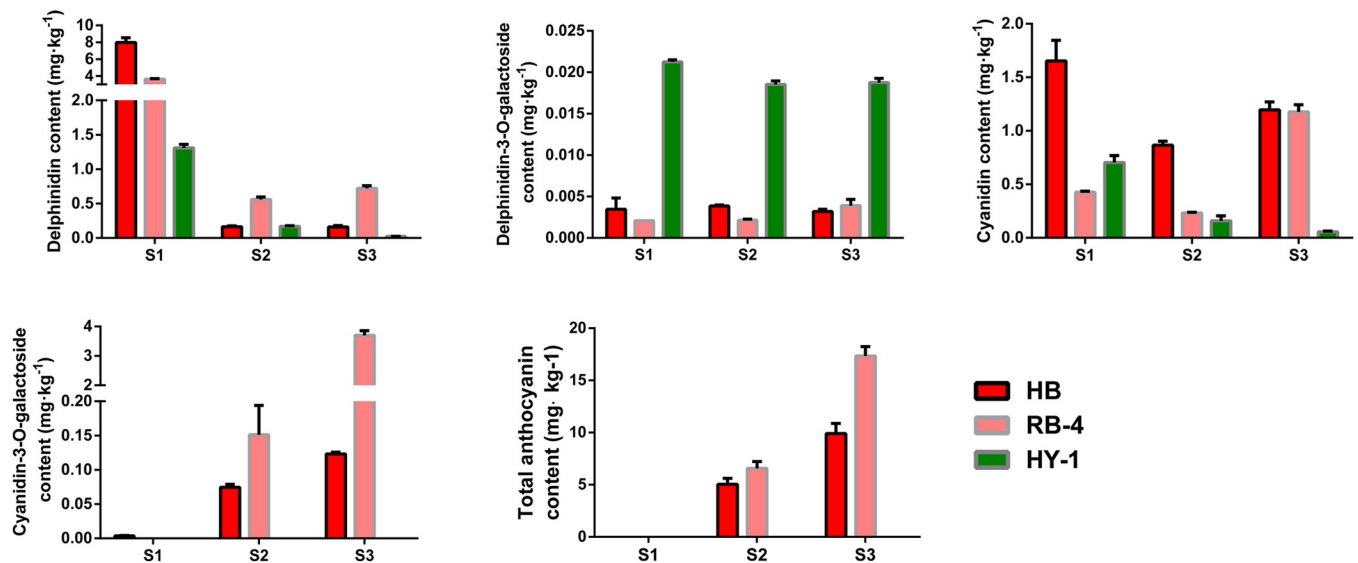


**Fig 5. Changes of four different typed anthocyanin and total anthocyanin content in the flesh of 'HB', 'RB-4' and 'HY-1' kiwifruit during three different developmental stages S1, S2 and S3.** Data are means SD of three replicates. Red, pink and green column represent 'HB', 'RB-4' and 'HY-1', respectively.

<https://doi.org/10.1371/journal.pone.0217480.g005>

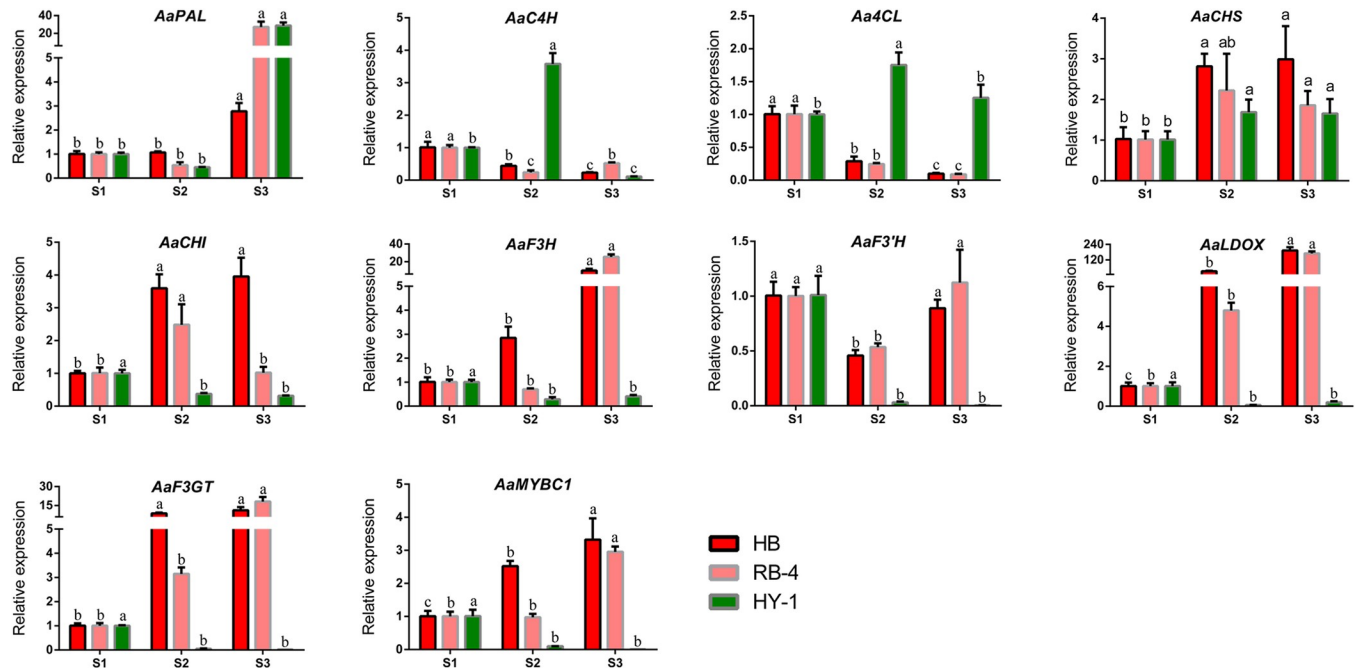


**Fig 6. Expression profiles of anthocyanin pathway genes at 3 stages (S1, S2 and S3) in 'HB', 'RB-4', and 'HY-1' kiwifruit.** The results represent the means SD of three replicates. Different lowercase letters indicate significant difference at  $P \leq 0.05$ .

<https://doi.org/10.1371/journal.pone.0217480.g006>

### Gene expression profiles, cluster and correlation analysis

On the basis of our previous transcriptome results, we used the sequenced coding DNA sequence (CDS) of *AaMYBC1* as well as 8 structural genes involved in anthocyanin biosynthesis for designing primers and performing qPCR (S8 Table). The results clearly showed that the expression levels of three structural genes (*AaF3H*, *AaLDOX* and *AaF3GT*) tended to increase from S1 to S3 and peaked at S3 in the two red-fleshed *A. arguta* cultivars 'HB' and 'RB-4'; however, the low expression trend of these genes was observed at S3 in the green-fleshed *A. arguta* cultivar contrasted with that in the red-fleshed ones. The same pattern was observed for *AaMYBC1* (Fig 6). The cluster analysis showed that the gene, *AaLDOX*, clustered into a single class in 'HB' (Fig 7A, S9 Table), which indicate that *AaLDOX* plays a key role in anthocyanin biosynthesis. Correlation analysis revealed that there was significant correlation between gene expression of *AaMYBC1* and cyanidin-3-O-galactoside content from S1 to S3 in 'HB' (Fig 7B, S10 Table). Together, these results suggested that *AaMYBC1* and *AaLDOX* played a key role in anthocyanin biosynthesis, which contributed to the fruit coloring in *A. arguta*. In addition, expression difference of miR858 between red-fleshed and green-fleshed kiwifruit showed that the expression level of miR858 was significant higher at S1 (green flesh) than S3 (red flesh) in 'HB' (Fig 8A), while there were no significant difference of miR858 expression at S1, S2 and S3 in 'HY-1' (Fig 8B), which validated the correctness of the sequencing results.

### The miRNA-target gene regulatory network of anthocyanin biosynthesis

To better understand the role of miRNAs involved in anthocyanin biosynthesis, all results were combined to establish a network to show the relationship between miRNAs and anthocyanin biosynthesis (Fig 9). The miR858 was identified in the present study as well as its target genes *AaMYBC1* which encodes a transcription factor. The expression level of miR858 gradually decreased from S1 to S3, while their targets gradually increased from S1 to S3. The

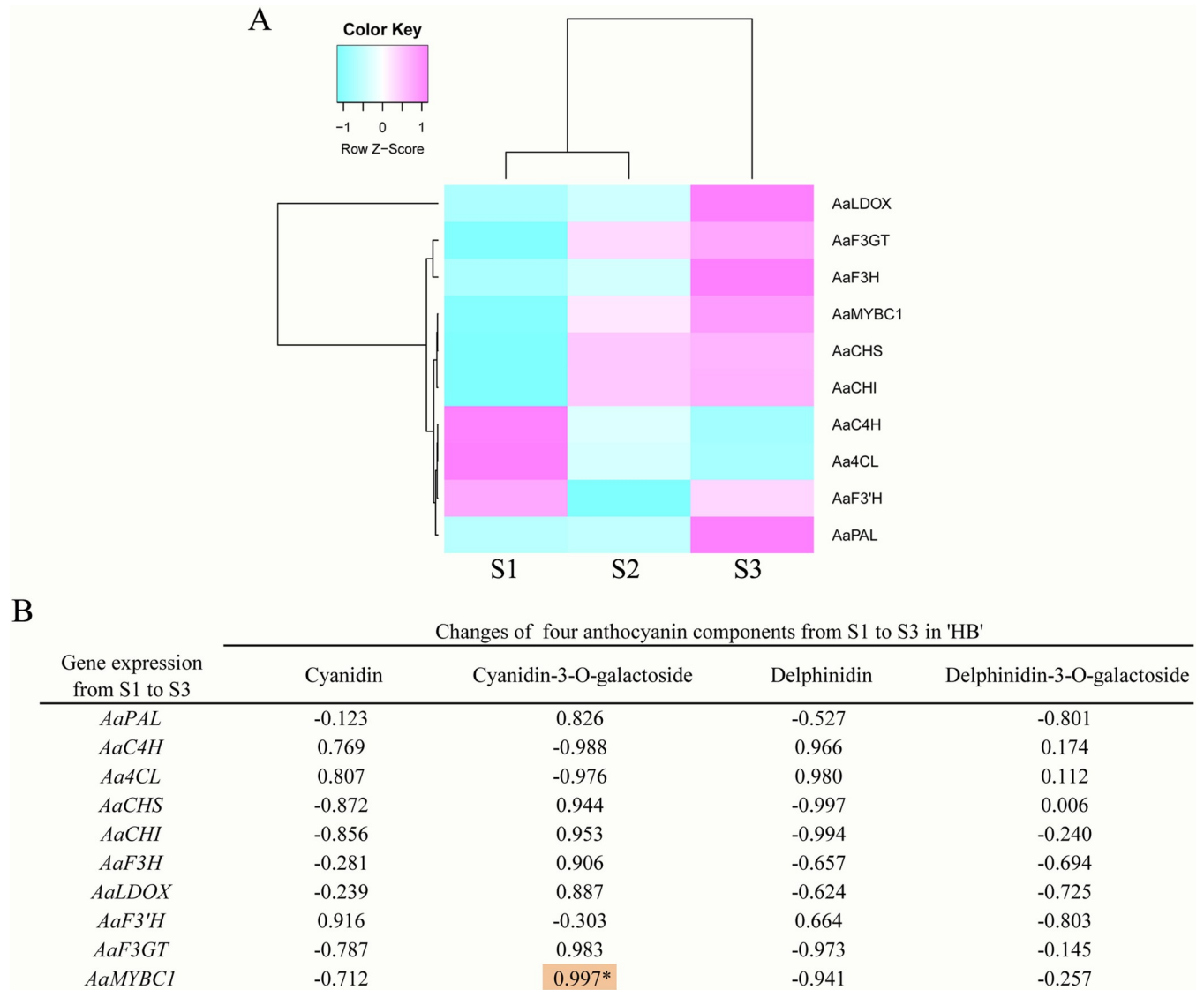


**Fig 7. Cluster and correlation analysis.** (A) Cluster analysis of gene expression in 'HB'; (B) Correlation analysis between content of four anthocyanin components and gene expression from S1 to S3 in 'HB'. The purple boxes indicate high expression levels, and the cyan boxes indicate low expression levels. \*\* indicates correlation is significant at 0.05 level.

<https://doi.org/10.1371/journal.pone.0217480.g007>

miRNA:target alignment showed that miR858 inhibit the expression of *AaMYBC1* by incomplete complement. Expression differences of *AaLDOX* regulated by transcription factor *AaMYBC1* resulted in content differences of four anthocyanin components in *A. arguta*, which leads to distinct fruit color. The proposed network would provide a new insight for revealing the red mechanism of *A. arguta*.

### Discussion

MiRNAs are important regulators involved in various biological processes, including biotic and abiotic stress tolerance, plant growth and development, metabolic pathways and morphogenesis. Extensive reports show that miRNAs regulate fruit development in multiple plants, including orange [50], pear [51], tomato [52], and persimmon [53]. Although many miRNAs

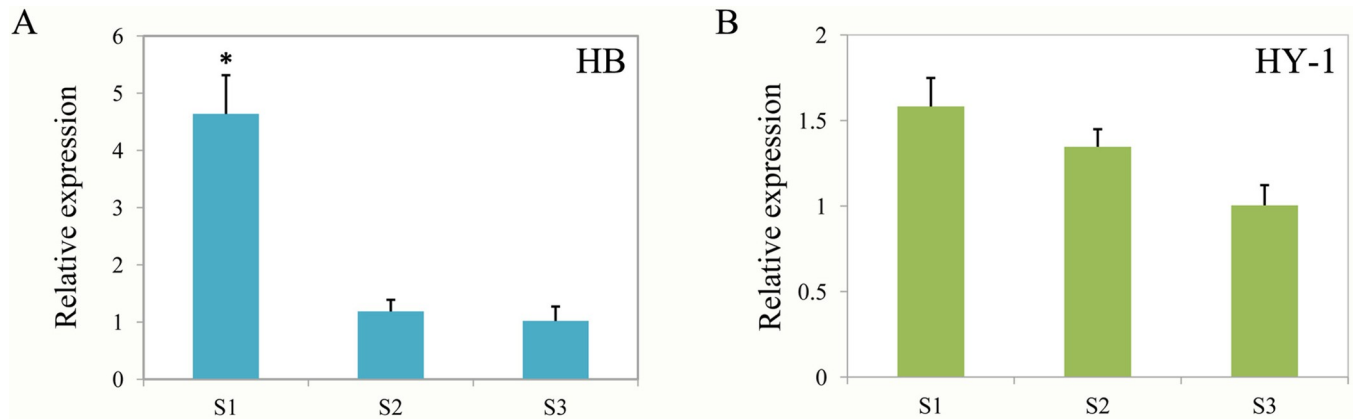


**Fig 8. Expression comparison of miR858 in red-fleshed 'HB' and green-fleshed 'HY-1' kiwifruit at three developmental stages.** (A) Expression level of miR858 in 'HB'. (B) Expression level of miR858 in 'HY-1'. The Results represent the means SD of three replicates. Data were analyzed with Student's t-test (\*P < 0.05).

<https://doi.org/10.1371/journal.pone.0217480.g008>

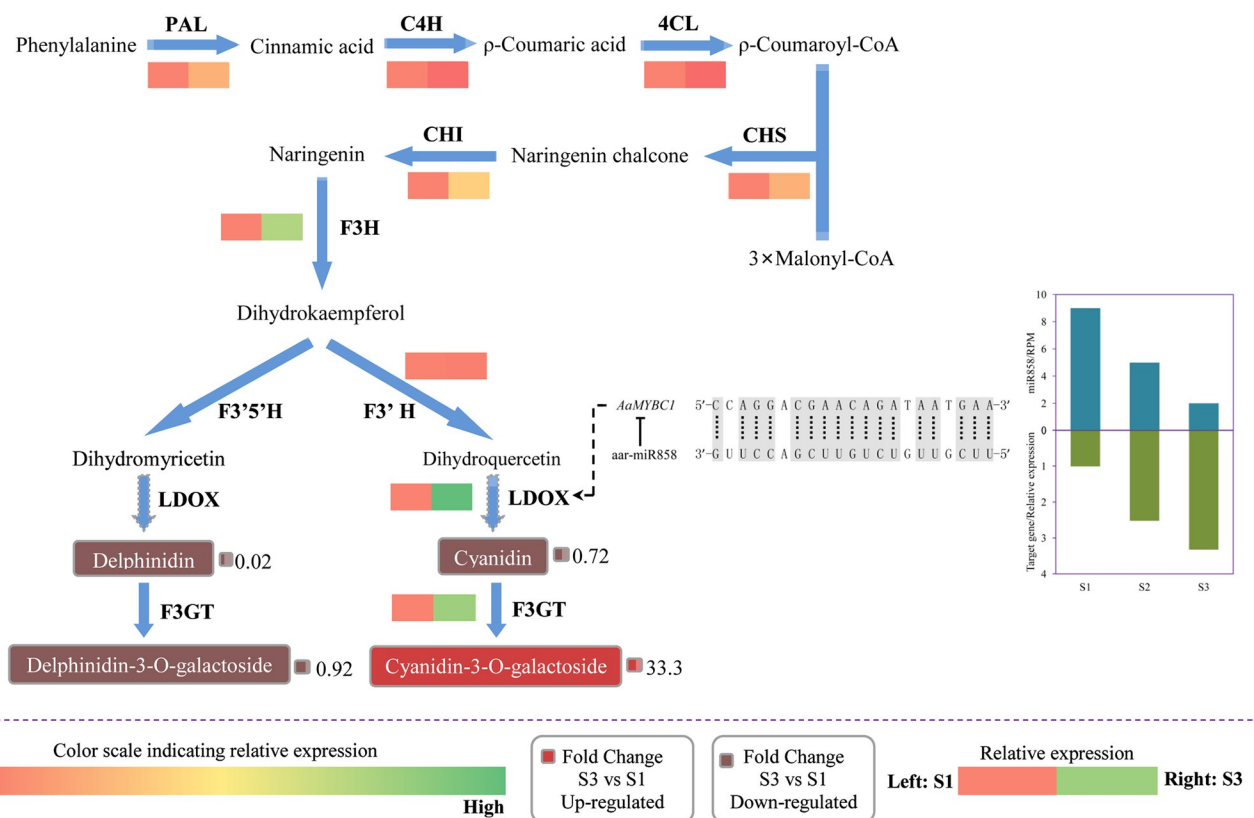


**Fig 9. *Actinidia arguta* miRNA-target gene regulatory network involved in anthocyanin biosynthesis at two development stages S3 and S1.** The right presentation showed the corresponding miRNA:target alignment and the expression levels of miR858 and its target gene from S1 to S3. T bar refer to negative role of miRNA on its target gene. Dotted arrow indicates indirect regulation of miRNA on anthocyanin biosynthesis. Color scale from red to green represent relative expression level from low to high. Small red and dark red grid represent up-regulated and down-regulated fold change of different anthocyanin components between S3 and S1, respectively. PAL, phenylalanine ammonia-lyase; C4H, trans-cinnamate 4-hydroxylase; 4CL, 4-coumarate: CoA ligase; CHS, Chalcone synthase; CHI, Chalcone isomerase; F3H, flavanone 3-hydroxylase; F3'H, flavonoid 3'-hydroxylase; LDOX, leucoanthocyanidin dioxygenase; F3GT, flavonoid 3-O-glucosyl-transferase.

<https://doi.org/10.1371/journal.pone.0217480.g009>

have been identified by small RNA sequencing in both model plants and many fruit trees including *Arabidopsis thaliana* [54], tomato [55], rice [56], apple [57] and peach [58], miRNAs have not been characterized in *A. arguta*. The results of our previous study suggests that anthocyanin accumulation in *A. arguta* during fruit development is accompanied by the expression of relevant gene, indicating that fruit coloring is both a dynamical process and a complex network regulated by a series of genes [48, 59]. Therefore, the identification of miRNAs in *A. arguta* can provide valuable information to better understand the biological process in fruit coloring.

### miRNAs were identified by small RNA sequencing

In this study, after removing any redundancy among 1,315 original miRNAs, we obtained 1,063 miRNAs, including 482 known miRNAs corresponding to 526 pre-miRNAs and 581 novel miRNAs corresponding to 619 pre-miRNAs, which were grouped into 46 miRNA families. (Table 2, S1 Table). In order to obtain functional information of miRNAs, the target genes of 321 identified miRNAs were identified and were used for further analysis of GO and KEGG pathway enrichment. A total of 814 and 207 target genes were assigned into three GO functional categories and 18 KEGG pathway terms (Fig3A, Fig 3B, S3–S6 Tables). To seek for miRNAs that are involved in anthocyanin synthesis, the comparison of S3 vs S1 was confirmed as cut-in spot for further analysis. Finally, we identified miR858 as a candidate miRNA and also found that its target gene *AaMYBC1* encoding a transcription factor is involved in anthocyanin biosynthesis.

### The content of four anthocyanin components

As important color pigments, anthocyanins are widely found in various plant species including kiwifruit. In this study, four different anthocyanin components and total anthocyanin content were measured in the flesh of three *A. arguta* cultivars at three developmental stages. The cyanidin-3-O-galactoside was detected in the red-fleshed *A. arguta* ‘HB’ and ‘RB-4’, but rarely in green-fleshed *A. arguta* ‘HY-1’ fruit (Fig 5). It indicates that the cyanidin-3-O-galactoside is the dominant chromogenic pigment in *A. arguta*, which contribute to color differences between red- and green-fleshed *A. arguta* cultivars. It provides evidence that this particular anthocyanin component plays a crucial role in fruit coloration in *A. arguta*. It is consistent with the results reported previous, in which the red color of the red-fleshed *A. arguta* is due to anthocyanin accumulation [47, 59–62].

### Key genes involved in anthocyanin biosynthesis

Gene expression is fundamental and indispensable to the integrity of biological processes. The spatio-temporal specificity of gene expression is deliberately controlled by transcription factors that are involved in sophisticated regulatory networks. In addition to transcription factors, the miRNAs and their target genes also exert considerable influence on the expression of downstream genes through modulating the regulatory network [63]. In plant species, extensive studies have suggested that anthocyanin biosynthesis is a sophisticated process which is regulated by multiple exogenous and endogenous factors, such as transcription factors [27]. Many transcription factors have been identified in kiwifruit. For example, *AcMYB110* is an R2R3 MYB that regulates the coloration of red petals in kiwifruit [64], and *AcMYBF110* is a crucial MYB that regulates anthocyanin biosynthesis in red kiwifruit [62]. In our study, *AaMYBC1* transcription factor is found to play a crucial role in anthocyanin biosynthesis in *A. arguta*. This suggests that the key transcription factors involved in anthocyanin biosynthesis might be different in different *Actinidia* species. Structural genes encoding enzymes that participate in

anthocyanin biosynthesis have been identified and cloned in kiwifruit [62, 65]. In our study, a structural gene *AaLDOX* was considered the key structural gene involved in anthocyanin biosynthesis in *A. arguta*, which is inconsistent with previous suggestions by which the formation of red inner pericarp of 'HD22' and 'Hongyang' results from high expression levels of *AcF3GT* and *UFGT*, respectively [62, 65]. This contradiction suggests that the structural genes regulating anthocyanin biosynthesis may differ among *Actinidia* species. The result of correlation analysis showed that expression of *AaMYBC1* at three stages was strongly correlated to anthocyanin content in *A. arguta* 'HB' (Fig 7), indicating that the *AaMYBC1* positively regulates anthocyanin biosynthesis, thereby we speculated that these two genes, *AaMYBC1* and *AaLDOX* play a key role in anthocyanin biosynthesis in *A. arguta*.

### Establishment of regulatory network model

In summary, the above mentioned results were combined to propose a model in which describes an association of miRNA and anthocyanin biosynthesis in *A. arguta* (Fig 9). When the fruit is green at S1, miR858 highly expresses and combines with its target gene *AaMYBC1* encoding *AaMYBC1* transcription factor that can act on promoter of *AaLDOX* structural gene. This combination indirectly suppresses the transcription of *AaLDOX*, which encode key enzymes that participate in anthocyanin biosynthesis. This suppression explains why the expression levels of *AaMYBC1* and *AaLDOX* are extremely low. However, when the fruit is red at S3, the expression level of miR858 is low while its target gene is high, the anthocyanin biosynthesis normally recover. As negative regulator, miR858 suppresses anthocyanin biosynthesis in *A. arguta*, which agree Jia et al. [28], who suggested miR858 is a negative regulator of anthocyanin biosynthesis in tomato, but disagree with those of Wang et al. [27], who suggested that, by repressing the expression of *MYBL2*, miR858a positively regulate anthocyanin biosynthesis in *Arabidopsis* seedlings. These finding suggest that miRNAs may serve distinct functions across species.

### Supporting information

#### S1 Fig. Pearson correlations between different samples.

(TIF)

#### S2 Fig. PLS-DA.

(TIF)

#### S3 Fig. UPLC profile results of different samples.

(TIF)

#### S1 Table. Relevant information on miRNA families.

(XLSX)

#### S2 Table. Relevant information on miRNAs in other species.

(XLSX)

#### S3 Table. Identified miRNAs whose expression significantly differ.

(XLSX)

#### S4 Table. Information on predicted target genes.

(XLSX)

#### S5 Table. GO analysis of target genes.

(XLSX)

**S6 Table. KEGG pathway analysis of target genes.**  
(XLSX)

**S7 Table. Annotation of target genes for 13 miRNAs.**  
(XLSX)

**S8 Table. Primer sequences of genes used for qRT-PCR.**  
(XLSX)

**S9 Table. Data used for cluster analysis.**  
(XLSX)

**S10 Table. Gene expression and content of anthocyanin components from S1 to S3 in 'HB'.**  
(XLSX)

## Author Contributions

**Conceptualization:** Miaomiao Lin, Yunpeng Zhong, Leiming Sun.

**Data curation:** Yukuo Li, Wen Cui, Ran Wang.

**Formal analysis:** Yukuo Li, Wen Cui, Ran Wang.

**Funding acquisition:** Xiujuan Qi, Jinbao Fang.

**Investigation:** Yukuo Li, Wen Cui.

**Methodology:** Yukuo Li, Wen Cui.

**Project administration:** Yukuo Li, Wen Cui.

**Resources:** Miaomiao Lin, Yunpeng Zhong, Leiming Sun.

**Software:** Miaomiao Lin, Yunpeng Zhong, Leiming Sun.

**Supervision:** Xiujuan Qi, Jinbao Fang.

**Validation:** Yukuo Li, Wen Cui.

**Writing – original draft:** Yukuo Li, Wen Cui.

**Writing – review & editing:** Yukuo Li, Wen Cui, Ran Wang, Xiujuan Qi, Jinbao Fang.

## References

1. Zhang Q, Liu CY, Liu YF, VanBuren R, Yao XH, Zhong CH, et al. High-density interspecific genetic maps of kiwifruit and the identification of sex-specific markers. *DNA Research*. 2015; 22(5): 367–375. <https://doi.org/10.1093/dnares/dsv019> PMID: 26370666
2. Chen YA, Yang H, Liu YF. GAP Production Technology in Kiwifruit. Yangling: Northwest A & F University Press. 2013.
3. Huang HW, Ferguson AR. *Actinidia* in China: Natural diversity, phylogeographical evolution, interspecific gene flow and kiwifruit cultivar improvement. *Acta horticulturae*. 2007; 753(753): 31–40. <https://doi.org/10.17660/ActaHortic.2007.753.1>
4. Zhang L, Li ZZ, Wang YC, Jiang ZW, Wang SM, Huang HW. Vitamin C, flower color and ploidy variation of hybrids from a ploidy-unbalanced *Actinidia* interspecific cross and SSR characterization. *Euphytica*. 2010; 175(1): 133–143. <https://doi.org/10.1007/s10681-010-0194-z>
5. Kovinich N, Kayanja G, Chanoca A, Riedl K, Otegui MS, Grotewold E. Not all anthocyanins are born equal: distinct patterns induced by stress in *Arabidopsis*. *Planta*. 2014; 240(5): 671–687. <https://doi.org/10.1007/s00425-014-2079-1> PMID: 24903357
6. Petroni K, Tonelli C. Recent advances on the regulation of anthocyanin synthesis in reproductive organs. *Plant science*. 2011; 181(3): 219–29. <https://doi.org/10.1016/j.plantsci.2011.05.009> PMID: 21763532

7. Jaakola L. New insights into the regulation of anthocyanin biosynthesis in fruits. *Trends in plant science*. 2013; 18(9): 477–83. <https://doi.org/10.1016/j.tplants.2013.06.003> PMID: 23870661
8. Tsuda T. Dietary anthocyanin-rich plants: biochemical basis and recent progress in health benefits studies. *Molecular nutrition & food research*. 2012; 56(1): 159–70. <https://doi.org/10.1002/mnfr.201100526> PMID: 22102523
9. Halliwell B. Dietary polyphenols: good, bad, or indifferent for your health? *Cardiovascular research*. 2007; 73(2): 341–7. <https://doi.org/10.1016/j.cardiores.2006.10.004> PMID: 17141749
10. Luceri C, Giovannelli L, Pitozzi V, Toti S, Castagnini C, Routaboul JM, et al. Liver and colon DNA oxidative damage and gene expression profiles of rats fed *Arabidopsis thaliana* mutant seeds containing contrasted flavonoids. *Food and chemical toxicology*. 2008; 46(4): 1213–20. <https://doi.org/10.1016/j.fct.2007.10.007> PMID: 18035473
11. Alipour B, Rashidkhani B, Edalati S. Dietary flavonoid intake, total antioxidant capacity and lipid oxidative damage: A cross-sectional study of Iranian women. *Nutrition*. 2015; 32(5): 566–72. <https://doi.org/10.1016/j.nut.2015.11.011> PMID: 26830011
12. Takos AM, Ubi BE, Robinson SP, Walker AR. Condensed tannin biosynthesis genes are regulated separately from other flavonoid biosynthesis genes in apple fruit skin. *Plant science*. 2006; 170(3): 487–499. <https://doi.org/10.1016/j.plantsci.2005.10.001>
13. Quattrocchio F, Wing JF, Leppen H, Mol J, Koes RE. Regulatory genes controlling anthocyanin pigmentation are functionally conserved among plant species and have distinct sets of target genes. *Plant cell*. 1993; 5(11): 1497–1512. <https://doi.org/10.1105/tpc.5.11.1497> PMID: 12271045
14. Holton TA, Cornish EC. Genetics and biochemistry of anthocyanin biosynthesis. *Plant cell*. 1995; 7(7): 1071–1083. <https://doi.org/10.1105/tpc.7.7.1071> PMID: 12242398
15. Song YH, Yoo CM, Hong AP, Kim SH, Jeong HJ, Shin SY, et al. DNA-binding study identifies C-Box and hybrid C/G-Box or C/ABox motifs as high-affinity binding sites for STF1 and LONG HYPO-COTYL5 proteins. *Plant physiology*. 2008; 146(4): 1862–77. <https://doi.org/10.1104/pp.107.113217> PMID: 18287490
16. Albert NW, Lewis DH, Zhang H, Schwinn KE, Jameson PE, Davies KM. Members of an R2R3-MYB transcription factor family in *Petunia* are developmentally and environmentally regulated to control complex floral and vegetative pigmentation patterning. *Plant journal*. 2011; 65(5): 771–784. <https://doi.org/10.1111/j.1365-3113X.2010.04465.x> PMID: 21235651
17. An XH, Tian Y, Chen KQ, Wang XF, Hao YJ. The apple WD40 protein MdTTG1 interacts with bHLH but not MYB proteins to regulate anthocyanin accumulation. *Journal of plant physiology*. 2012; 169(7): 710–7. <https://doi.org/10.1016/j.jplph.2012.01.015> PMID: 22405592
18. Schaart JG, Dubos C, Romero De La Fuente I, van Houwelingen AM, de Vos RC, Jonker HH, et al. Identification and characterization of MYB-bHLH-WD40 regulatory complexes controlling proanthocyanidin biosynthesis in strawberry (*Fragaria × ananassa*) fruits. *New phytologist*. 2012; 197(2): 454–67. <https://doi.org/10.1111/nph.12017> PMID: 23157553
19. Patra B, Schluttenhofer C, Wu Y, Pattanaik S, Yuan L. Transcriptional regulation of secondary metabolite biosynthesis in plants. *Biochimica et biophysica acta*. 2013; 1829(11): 1236–47 <https://doi.org/10.1016/j.bbagr.2013.09.006> PMID: 24113224
20. Li W, Wang B, Wang M, Chen M, Yin JM, Kaleri GM, et al. Cloning and characterization of a potato StAN11 gene involved in anthocyanin biosynthesis regulation. *Journal of integrative plant biology*. 2014; 56(4): 364–72. <https://doi.org/10.1111/jipb.12136> PMID: 24304603
21. Xu W, Grain D, Bobet S, Le Gourrierc J, Thévenin J, Kelemen Z, et al. Complexity and robustness of the flavonoid transcriptional regulatory network revealed by comprehensive analyses of MYB-bHLH-WDR complexes and their targets in *Arabidopsis* seed. *New phytologist*. 2014; 202(1): 132–144. <https://doi.org/10.1111/nph.12620> PMID: 24299194
22. Montefiori M, Brendolise C, Dare AP, Wang KL, Davies KM, Hellens RP, et al. In the Solanaceae, a hierarchy of bHLHs confer distinct target specificity to the anthocyanin regulatory complex. *Journal of experimental botany*. 2015; 66(5): 1427–1436 <https://doi.org/10.1093/jxb/eru494> PMID: 25628328
23. Xu W, Dubos C, Lepiniec L. Transcriptional control of flavonoid biosynthesis by MYB-bHLH-WDR complexes. *Trends in plant science*. 2015; 20(3): 176–85. <https://doi.org/10.1016/j.tplants.2014.12.001> PMID: 25577424
24. El-Sharkawy I, Liang D, Xu KN. Transcriptome analysis of an apple (*Malus × domestica*) yellow fruit somatic mutation identifies a gene network module highly associated with anthocyanin and epigenetic regulation. *Journal of experimental botany*. 2015; 66(22): 7359–76. <https://doi.org/10.1093/jxb/erv433> PMID: 26417021
25. Cho K, Cho KS, Sohn HB, Ha IJ, Hong SY, Lee H, et al. Network analysis of the metabolome and transcriptome reveals novel regulation of potato pigmentation. *Journal of experimental botany*. 2016; 67(5): 1519–33. <https://doi.org/10.1093/jxb/erv549> PMID: 26733692

26. Testolin R, Huang HW, Ferguson AR. The Kiwifruit Genome. Publisher: Springer. 2016.
27. Wang YL, Wang YQ, Song ZQ, Zhang HY. Repression of MYBL2 by Both microRNA858a and HY5 Leads to the Activation of Anthocyanin Biosynthetic Pathway in *Arabidopsis*. *Molecular plant*. 2016; 9(10): 1395–1405. <https://doi.org/10.1016/j.molp.2016.07.003> PMID: 27450422
28. Jia X, Shen J, Liu H, Li F, Ding N, Gao C, et al. Small tandem target mimic-mediated blockage of microRNA858 induces anthocyanin accumulation in tomato. *Planta*. 2015; 242(1): 283–93. <https://doi.org/10.1007/s00425-015-2305-5> PMID: 25916310
29. Rhoades MW, Reinhart BJ, Lim LP, Burge CB, Bartel B, Bartel DP. Prediction of plant microRNA targets. *Cell*. 2002; 110(4): 513–20. [https://doi.org/10.1016/S00928674\(02\)00863-2](https://doi.org/10.1016/S00928674(02)00863-2) PMID: 12202040
30. Jones-Rhoades MW, Bartel DP, Bartel B. MicroRNAs and their regulatory roles in plants. *Annual review of plant biology*. 2006; 57: 19–53. <https://doi.org/10.1146/annurev.arplant.57.032905.105218> PMID: 16669754
31. Matzke M, Kanno T, Daxinger L, Huetzel B, Matzke AJ. RNA-mediated chromatin-based silencing in plants. *Current opinion in cell biology*. 2009; 21(3): 367–76. <https://doi.org/10.1016/j.ceb.2009.01.025> PMID: 19243928
32. Gou JY, Felippes FF, Liu CJ, Weigel D, Wang JW. Negative regulation of anthocyanin biosynthesis in *Arabidopsis* by a miR156-targeted SPL transcription factor. *Plant cell*. 2011; 23(4): 1512–22. <https://doi.org/10.1105/tpc.111.084525> PMID: 21487097
33. Xia R, Zhu H, An YQ, Beers EP, Liu Z. Apple miRNAs and tasiRNAs with novel regulatory networks. *Genome Biology*. 2012; 13(6): R47. <https://doi.org/10.1186/gb-2012-13-6-r47> PMID: 22704043
34. Zhang H, He H, Wang X, Wang X, Yang X, Li L, et al. Genome-wide mapping of the HY5-mediated gene networks in *Arabidopsis* that involve both transcriptional and post-transcriptional regulation. *Plant journal*. 2011; 65(3): 346–58. <https://doi.org/10.1111/j.1365-313X.2010.04426.x> PMID: 21265889
35. Zhang H, Zhao X, Li J, Cai H, Deng XW, Li L. MicroRNA408 is critical for the HY5-SPL7 gene network that mediates the coordinated response to light and copper. *Plant cell*. 2014; 26(12): 4933–53. <https://doi.org/10.1105/tpc.114.127340> PMID: 25516599
36. Hsieh LC, Lin SI, Shih AC, Chen JW, Lin WY, Tseng CY, et al. Uncovering small RNA-mediated responses to phosphate deficiency in *Arabidopsis* by deep sequencing. *Plant physiology*. 2009; 151(4): 2120–32. <https://doi.org/10.1104/pp.109.147280> PMID: 19854858
37. Luo QJ, Mittal A, Jia F, Rock CD. An autoregulatory feedback loop involving PAP1 and TAS4 in response to sugars in *Arabidopsis*. *Plant molecular biology*. 2012; 80(1): 117–29. <https://doi.org/10.1007/s11103-011-9778-9> PMID: 21533841
38. Yang F, Cai J, Yang Y, Liu Z. Overexpression of microRNA828 reduces anthocyanin accumulation in *Arabidopsis*. *Plant cell tissue & organ culture*. 2013; 115(2): 159–167. <https://doi.org/10.1007/s11240-013-0349-4>
39. Varkonyi-Gasic E, Lough RH, Moss SM, Wu R, Hellens RP. Kiwifruit floral gene APETALA2 is alternatively spliced and accumulates in aberrant indeterminate flowers in the absence of miR172. *Plant molecular biology*. 2012; 78(4–5): 417–29. <https://doi.org/10.1007/s11103-012-9877-2> PMID: 22290408
40. Langfelder F, Horvath S. WGCNA: an R package for weighted correlation network analysis. *BMC bioinformatics*. 2008; 9: 559. <https://doi.org/10.1186/1471-2105-9-559> PMID: 19114008
41. Zhou L, Chen JH, Li ZZ, Li XX, Hu XH, Huang Y, et al. Integrated profiling of microRNAs and mRNAs: microRNAs located on Xq27.3 associate with clear cell renal cell carcinoma. *Plos one*. 2010; 5(12): e15224. <https://doi.org/10.1371/journal.pone.0015224> PMID: 21253009
42. Wang L, Feng Z, Wang X, Wang X, Zhang X. DEGseq: an R package for identifying differentially expressed genes from RNA-seq data. *Bioinformatics*. 2010; 26(1): 136–8. <https://doi.org/10.1093/bioinformatics/btp612> PMID: 19855105
43. Bo X, Wang S. TargetFinder: a software for antisense oligonucleotide target site selection based on MAST and secondary structures of target mRNA. *Bioinformatics*. 2005; 21(8): 1401–2. <https://doi.org/10.1093/bioinformatics/bti211> PMID: 15598838
44. Young MD, Wakefield MJ, Smyth GK, Oshlack A. Gene ontology analysis for RNA-seq: accounting for selection bias. *Genome biology*. 2010; 11(2): R14. <https://doi.org/10.1186/gb-2010-11-2-r14> PMID: 20132535
45. Mao X, Cai T, Olyarchuk JG, Wei L. Automated genome annotation and pathway identification using the KEGG Orthology (KO) as a controlled vocabulary. *Bioinformatics*. 2005; 21: 3787–93. <https://doi.org/10.1093/bioinformatics/bti430> PMID: 15817693
46. Yang J, Jiang ZW, Wang YC. Cloning and expression of dihydroflavonol 4-reductase in *Actinidia chinensis* var. *rufopulpa*. *Journal of wuhan botany research*. 2010; 28: 673–681. <https://doi.org/10.3724/SP.J.1142.2010.60673>

47. Li Y, Fang J, Qi X, Lin M, Zhong Y, Sun L. A key structural gene, *AaLDOX*, is involved in anthocyanin biosynthesis in all red-fleshed kiwifruit (*Actinidia arguta*) based on transcriptome analysis. 2018; *Gene*. 648: 31–41. <https://doi.org/10.1016/j.gene.2018.01.022> PMID: 29309888
48. Livak KJ, Schmittgen TD. Analysis of relative gene expression data using real-time quantitative PCR and the  $2^{-\Delta\Delta CT}$  method. *Methods*. 2001; 25: 402–8. <https://doi.org/10.1006/meth.2001.1262> PMID: 11846609
49. Dheilly NM, Jouaux A, Boudry P, Favrel P, Lelong C. Hierarchical clustering using Pearson's correlation was performed using TMeV 4.6.0 software on the statistically significant transcripts (one-way ANOVA parametric test with a p-value cut-off of 0.01 and Bonferroni adjustment). *Plos one*. 2014.
50. Xu Q, Liu Y, Zhu A, Wu X, Ye J, Yu K, et al. Discovery and comparative profiling of microRNAs in a sweet orange red-flesh mutant and its wild type. *BMC genomics*. 2010; 11: 246. <https://doi.org/10.1186/1471-2164-11-246> PMID: 20398412
51. Wu J, Wang D, Liu Y, Wang L, Qiao X, Zhang S. Identification of miRNAs involved in pear fruit development and quality. *BMC genomics*. 2014; 15: 953. <https://doi.org/10.1186/1471-2164-15-953> PMID: 25366381
52. Chen W, Kong J, Lai T, Manning K, Wu C, Wang Y, et al. Tuning LeSPL-CNR expression by SlymiR157 affects tomato fruit ripening. *Scientific reports*. 2015; 5: 7852. <https://doi.org/10.1038/srep07852> PMID: 25597857
53. Luo Y, Zhang X, Luo Z, Zhang Q, Liu J. Identification and characterization of microRNAs from Chinese pollination constant non-astringent persimmon using high-throughput sequencing. *BMC plant biology*. 2015; 15: 11. <https://doi.org/10.1186/s12870-014-0400-6> PMID: 25604351
54. Qi XP, Bao FS, Xie ZX. Small RNA Deep Sequencing Reveals Role for Arabidopsis thaliana RNA-Dependent RNA Polymerases in Viral siRNA Biogenesis. *Plos one*. 2009; 4(4): e4971. <https://doi.org/10.1371/journal.pone.0004971> PMID: 19308254
55. Xu T, Wang Y, Liu X, Lv S, Feng C, Qi M, et al. Small RNA and degradome sequencing reveals microRNAs and their targets involved in tomato pedicel abscission. *Planta*. 2015; 242(4): 963–84. <https://doi.org/10.1007/s00425-015-2318-0> PMID: 26021606
56. Zhou M, Gu LF, Li PC, Song XW, Wei LY, Chen ZY, et al. Degradome sequencing reveals endogenous small rna targets in rice (*oryza sativa* L. ssp. *indica*). *Frontiers in biology*. 2010; 5(1): 67–90. <https://doi.org/10.1007/s11515-010-0007-8>
57. Guo X, Ma Z, Zhang Z, Cheng L, Zhang X, Li T. Small rna-sequencing links physiological changes and rddm process to vegetative-to-floral transition in apple. *Frontiers in plant science*. 2017; 8: 873. <https://doi.org/10.3389/fpls.2017.00873> PMID: 28611800
58. Zhang CH, Zhang BB, Ma RJ, Yu ML, Guo SL, Guo L. Identification of known and novel micrnas and their targets in peach (*prunus persica*) fruit by high-throughput sequencing. *Plos one*. 2016; 11, e0159253. <https://doi.org/10.1371/journal.pone.0159253> PMID: 27466805
59. Li Y, Fang J, Qi X, Lin M, Zhong Y, Sun L, et al. Combined Analysis of the Fruit Metabolome and Transcriptome Reveals Candidate Genes Involved in Flavonoid Biosynthesis in *Actinidia arguta*. 2018; *International Journal of Molecular Sciences*. 19, 1471. <https://doi.org/10.3390/ijms19051471> PMID: 29762529
60. Li W, Liu Y, Zeng S, Xiao G, Wang G, Wang Y, et al. Gene expression profiling of development and anthocyanin accumulation in kiwifruit (*Actinidia chinensis*) based on transcriptome sequencing. *Plos one*. 2015; 10(8): e0136439. <https://doi.org/10.1371/journal.pone.0136439> PMID: 26301713
61. Man YP, Wang YC, Li ZZ, Jiang ZW, Yang HL, Gong JJ, et al. High-temperature inhibition of biosynthesis and transportation of anthocyanins results in the poor red coloration in red-fleshed *Actinidia chinensis*. *Physiologia plantarum*. 2015; 153: 565–583. <https://doi.org/10.1111/ppl.12263> PMID: 25143057
62. Liu Y, Zhou B, Qi Y, Chen X, Liu C, Liu Z, et al. Expression differences of pigment structural genes and transcription factors explain flesh coloration in three contrasting kiwifruit cultivars. *Frontiers in plant science*. 2017; 8: 1507. <https://doi.org/10.3389/fpls.2017.01507> PMID: 28919902
63. Voinnet O. Origin, Biogenesis, and Activity of Plant MicroRNAs. *Cell*. 2009; 136(4): 669–87. <https://doi.org/10.1016/j.cell.2009.01.046> PMID: 19239888
64. Fraser LG, Seal AG, Montefiori M, McGhie TK, Tsang GK, Datson PM, et al. An R2R3 MYB transcription factor determines red petal colour in an *Actinidia* (kiwifruit) hybrid population. *BMC genomics*. 2013; 14: 28. <https://doi.org/10.1186/1471-2164-14-28> PMID: 23324587
65. Montefiori M, Espley RV, Stevenson D, Cooney J, Datson PM, Saiz A, et al. Identification and characterisation of F3GT1 and F3GGT1, two glycosyltransferases responsible for anthocyanin biosynthesis in red-fleshed kiwifruit (*Actinidia chinensis*). *Plant journal*. 2011; 65(1): 106–118. <https://doi.org/10.1111/j.1365-3113X.2010.04409.x> PMID: 21175894